

# Optimal synchronization of complex networks

Per Sebastian Skardal,<sup>1,2,\*</sup> Dane Taylor,<sup>2,3,4,†</sup> and Jie Sun<sup>5,‡</sup>

<sup>1</sup>Departament d'Enginyeria Informàtica i Matemàtiques, Universitat Rovira i Virgili, 43007 Tarragona, Spain

<sup>2</sup>Department of Applied Mathematics, University of Colorado at Boulder, Colorado 80309, USA

<sup>3</sup>Statistical and Applied Mathematical Sciences Institute, Research Triangle Park, NC 27709, USA

<sup>4</sup>Department of Mathematics, University of North Carolina, Chapel Hill, NC 27599, USA

<sup>5</sup>Department of Mathematics, Clarkson University, Potsdam, NY 13699, USA

We study optimal synchronization in networks of heterogeneous phase oscillators. Our main result is the derivation of a *synchrony alignment function* that encodes the interplay between network structure and oscillators' frequencies and can be readily optimized. We highlight its utility in two general problems: constrained frequency allocation and network design. In general, we find that synchronization is promoted by strong alignments between frequencies and the dominant Laplacian eigenvectors, as well as a qualitative matching between the heterogeneity of frequencies and network structure.

PACS numbers: 05.45.Xt, 89.75.Hc

A central goal of complexity theory is to understand the emergence of collective behavior in large ensembles of interacting dynamical systems. Synchronization of network-coupled oscillators has served as a paradigm for understanding emergence [1–4], where examples arise in nature (e.g., flashing of fireflies [5] and cardiac pacemaker cells [6]), engineering (e.g., power grid [7] and bridge oscillations [8]), and at their intersection (e.g., synthetic cell engineering [9]). We consider the dynamics of  $N$  network-coupled phase oscillators  $\theta_i$  for  $i = 1, \dots, N$ , whose evolution is governed by

$$\dot{\theta}_i = \omega_i + K \sum_{j=1}^N A_{ij} H(\theta_j - \theta_i). \quad (1)$$

Here  $\omega_i$  is the natural frequency of oscillator  $i$ ,  $K > 0$  is the coupling strength,  $[A_{ij}]$  is the network adjacency matrix, and  $H$  is a  $2\pi$ -periodic coupling function [10]. The choices  $H(\theta) = \sin(\theta)$  and  $H(\theta) = \sin(\theta - \alpha)$  with the phase-lag parameter  $\alpha \in (0, \pi/2)$  yield the classical Kuramoto and Sakaguchi-Kuramoto models, respectively [11, 12]. Here we treat  $H(\theta)$  with full generality so long as  $H'(0) > 0$ .

Considerable research has shown that the underlying structure of a network plays a crucial role in determining its synchronizability [13–22], yet the precise relationship between the dynamical and structural properties of a network and its synchronization remains not fully understood. One unanswered question of interest to theorists and engineers alike is, given an objective measure of synchronization, how can synchronization be *optimized*? One application lies in synchronizing the power grid [23], where sources and loads can be modeled as oscillators with different frequencies. To this end, we ask the following question: what structural and/or dynamical properties should be present to optimize synchronization?

We measure the degree of synchronization of an ensemble of oscillators using the Kuramoto order parameter

$$re^{i\psi} = \frac{1}{N} \sum_{j=1}^N e^{i\theta_j}. \quad (2)$$

Here  $re^{i\psi}$  denotes the phases' centroid on the complex unit circle, with the magnitude  $r$  ranging from 0 (incoherence) to 1 (perfect synchronization) [11]. In general, the question of optimization (e.g., maximizing  $r$ ) is challenging due to the fact that the macroscopic system dynamics depend on both the dynamics of individual units (i.e., the natural frequencies) and the structure of the network (i.e., the adjacency matrix). To quantify the interplay between node dynamics and network structure, we derive directly from Eqs. (1) and (2) a *synchrony alignment function* which serves as an objective measure of synchronization and can be used to systematically optimize a network's synchronizability. We highlight this result by addressing two classes of optimization problem, which can be easily adapted to a wide range of applications. The first is *constrained frequency allocation*, where given a fixed network topology, optimal frequencies are chosen. The second is *network design*, where given a fixed set of frequencies, an optimal network is found. We next present the derivation of the synchrony alignment function. No assumptions are made about the frequencies or network structure aside from the network being connected and undirected.

We begin by considering the dynamics of Eq. (1) in the strong coupling regime where  $r \approx 1$ . In this regime the oscillators are entrained in a tight cluster such that  $\theta_i \approx \theta_j$  for all  $(i, j)$  pairs, so that expanding Eq. (1) yields

$$\dot{\theta}_i \approx \tilde{\omega}_i - K \sum_{j=1}^N L_{ij} \theta_j, \quad (3)$$

where  $\tilde{\omega}_i = \omega_i + KH(0)d_i$ ,  $d_i = \sum_{j=1}^N A_{ij}$  is the degree of node  $i$ , and  $[L_{ij}]$  is the Laplacian matrix whose entries are defined as  $L_{ij} = \delta_{ij}d_i - (1 - \delta_{ij})A_{ij}$ .

The following spectral properties of the Laplacian are essential to our analysis. First, since the network is connected and undirected, all the eigenvalues of  $L$  are real and can be ordered as  $0 = \lambda_1 < \lambda_2 \leq \dots \leq \lambda_{N-1} \leq \lambda_N$ . Second, the normalized eigenvectors  $\{\mathbf{v}^i\}_{i=1}^N$  form an orthonormal basis for  $\mathbb{R}^N$ . Furthermore, the eigenvector associated with  $\lambda_1 = 0$

is  $v^1 = 1$ , which corresponds to the synchronization manifold.

Inspecting Eq. (3) and entering the rotating frame  $\theta_i \mapsto \theta_i + \Omega t$  where  $\Omega = \langle \omega \rangle + KH(0)\langle \mathbf{d} \rangle$ , we find that if a steady-state solution  $\theta^*$  exists, it is given by

$$\theta^* = L^\dagger \tilde{\omega} / KH'(0), \quad (4)$$

where  $L^\dagger = \sum_{j=2}^N \lambda_j^{-1} v^j v^{jT}$  is the pseudo-inverse of  $L$  [24]. We next consider the order parameter for such a steady-state solution  $\theta^*$ . First, with a suitable shift in initial conditions the average phase can be set to zero, implying that the sum in Eq. (2) is real. Furthermore, in the strongly synchronized regime all phases are tightly packed about  $\psi = 0$ , thus  $|\theta_j^*| \ll 1$  for all  $n$ . Expanding Eq. (2) yields

$$r \approx 1 - \|\theta^*\|^2 / 2N. \quad (5)$$

Finally, we use the definition of the pseudo-inverse, take the norm of Eq. (4), and insert this into Eq. (5) to obtain

$$r = 1 - J(\tilde{\omega}, L) / 2K^2 H'^2(0), \quad (6)$$

for which we define the synchrony alignment function

$$J(\tilde{\omega}, L) = \frac{1}{N} \sum_{j=2}^N \lambda_j^{-2} \langle v^j, \tilde{\omega} \rangle^2. \quad (7)$$

The derivation of  $J(\tilde{\omega}, L)$  is our main theoretical result as its minimization corresponds to the maximization of the order parameter  $r$ , which allows for the optimization of synchronization using elementary properties of the network (i.e., Laplacian eigenvalues and eigenvectors) and the oscillators (i.e., the frequency vector). Before exploring the optimization of  $J(\tilde{\omega}, L)$ , we note the following interesting results. For  $H(0) = 0$  [e.g., the Kuramoto model  $H(\theta) = \sin(\theta)$ ], it follows that  $\tilde{\omega} = \omega$ , and thus optimization of  $J(\omega, L)$  is independent of  $K$ . However, for  $H(0) \neq 0$  perfect synchrony,  $r = 1$ , is not attainable since in the limit  $K \rightarrow \infty$  Eq. (6) yields  $r = 1 - J(\mathbf{d}, L)H^2(0)/2H'^2(0)$ . It follows that the existence of a strong coupling regime  $r \lesssim 1$  and consequently the approximations in our theory are valid only when  $J(\mathbf{d}, L)H^2(0)/2H'^2(0) \ll 1$ . Furthermore, since  $\tilde{\omega}$  depends on the coupling strength  $K$ , so will the optimization of  $J(\tilde{\omega}, L)$  and therefore the optimal network. From now on, we will specialize to the widely used Kuramoto model,  $H(\theta) = \sin(\theta)$ , although we emphasize that similar results are found for more general coupling functions  $H(\theta)$ .

We first address constrained frequency allocation for a fixed network. We note that by entering a rotating frame we can without loss of generality set the mean frequency  $\langle \omega \rangle$  to zero. Furthermore, the choice  $\omega = [0, \dots, 0]^T$  trivially minimizes Eq. (7), resulting in  $r = 1$ , so we require as a first constraint that  $\omega$  has a fixed standard deviation,  $\sigma = \sqrt{N^{-1} \sum_i \omega_i^2}$ . By rescaling time and the coupling strength,  $\sigma$  can be tuned freely, so without loss of generality we set  $\sigma = 1$ . To mini-

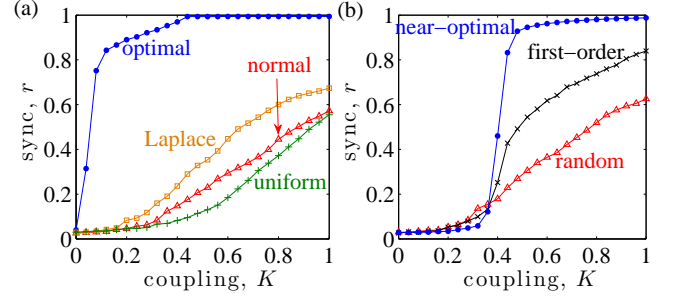


FIG. 1. (Color online) Constrained frequency allocation: (a)  $r$  vs  $K$  for optimal allocation (blue circles) compared with random allocations drawn from normal (red triangles), uniform (green pluses), and Laplace (orange squares) distributions. (b)  $r$  vs  $K$  for a pre-chosen set of normally distributed frequencies with random (red triangles), first-order (black crosses), and near-optimal (blue circles) arrangements. The near-optimal arrangement was obtained from  $S = 10^6$  proposed frequency exchanges. Networks are SF with  $N = 1000$ ,  $\gamma = 3$ , and  $d_0 = 2$ .

mize  $J(\omega, L)$ , we first express  $\omega$  as a linear combination of the nontrivial eigenvectors of  $L$ ,  $\omega = \sum_{i=2}^N \alpha_i v^i$ , where the coefficients must satisfy  $\sum_{i=2}^N \alpha_i^2 = N$ . After inserting this representation of  $\omega$  into Eq. (7) it follows that  $J(\omega, L)$  is minimized by the choice  $\alpha_2, \dots, \alpha_{N-1} = 0$  and  $\alpha_N = \sqrt{N}$ , yielding  $r = 1 - 1/2\lambda_N^2 K^2$ . Physically, this corresponds to aligning  $\omega$  with the dominant eigenvector  $v^N$ .

In Fig. 1 (a) we compare the results of optimal allocation,  $\omega = \sqrt{N} v^N$ , with several random frequency allocations by plotting the synchrony profiles  $r$  vs  $K$  for the optimal allocation, and those for frequencies randomly drawn from normal, uniform, and Laplace distribution (each with unit standard deviation). The underlying network with  $N = 1000$  nodes was constructed using the configuration model [25] with a scale-free (SF) degree distribution  $P(d) \propto d^{-\gamma}$  for  $\gamma = 3$  and minimum degree  $d_0 = 2$ . The optimal allocation shows a large improvement over all random alignments and is marked by a sharp transition to a strongly synchronized state at a small coupling strength. We note that two mechanisms contribute to the excellent performance of the optimal allocation: the choice of frequencies and the nodes to which they are assigned.

To elucidate the importance of these two different mechanisms, we consider an additional constraint where frequencies  $\{\omega_i\}_{i=1}^N$  are pre-chosen and must be arranged optimally on the network to minimize  $J(\omega, L)$ . Finding the global minimum requires an exhaustive search over all  $N!$  possible arrangements of  $\omega$  – an unrealistic option even for moderately sized networks. We therefore provide two alternatives: a *first-order* approximation applicable for networks in which the largest Laplacian eigenvalue  $\lambda_N$  is well separated from the others (often the case for real world and SF networks [26]) and a *near-optimal* solution based on an accept/reject algorithm. In particular, when the dominant eigenvalue is well separated,  $\lambda_i \ll \lambda_N$  for  $i \neq N$ , an inexpensive first-order minimization of the objective function leads to maximizing

$|\langle v^N, \omega \rangle|$ . This can be done simply by finding the index permutations  $i_1, \dots, i_N$  and  $j_1, \dots, j_N$  that place eigenvector entries in ascending order,  $v_{i_1}^N \leq \dots \leq v_{i_N}^N$ , and frequencies in ascending (or descending) order,  $\omega_{j_1} \leq \dots \leq \omega_{j_N}$  (or  $\omega_{j_1} \geq \dots \geq \omega_{j_N}$ ). In principle both pairings must be checked to select the best result, but typically yield comparable results. To find the near-optimal arrangement we begin with an initial arrangement  $\omega$  and construct a new arrangement  $\omega'$  by exchanging two randomly chosen entries. If  $J(\omega', L) < J(\omega, L)$  we accept  $\omega'$ , otherwise we reject it. This procedure is then repeated for  $S$  proposed exchanges.

In Fig. 1 (b) we compare synchronization profiles for the near-optimal and first-order arrangements to a random placement of frequencies drawn from the unit normal distribution. As expected, the near-optimal arrangement yields the best results, however, the first-order arrangement also performs well, providing an inexpensive way to improve upon purely random arrangements. These results also allow us to compare the potential of arranging pre-chosen frequencies and choosing frequencies freely under the constraint of a set standard deviation [recall Fig. 1 (a)]. In both cases, the transition from incoherence to strong synchronization is sharp, however it occurs at a larger coupling strength ( $K \approx 0.4$ ) when frequencies are pre-chosen, yielding two distinct regimes: for small  $K$  strong synchronization is only attainable when frequencies are freely tunable, while for larger  $K$  strong synchronization is attainable even when the frequency set is fixed.

Next we address the complimentary problem of optimal network design for a fixed set of frequencies. Given  $\omega$  and a fixed number of links, we look for a network that minimizes  $J(\omega, L)$ . As an algorithmic method for obtaining an approximate solution, we initialize an accept/reject algorithm with a network satisfying these constraints, and allow it to evolve as follows. A new network with Laplacian matrix  $L'$  is constructed by randomly deleting a link and introducing another between two previously disconnected nodes. If  $J(\omega, L') < J(\omega, L)$  we accept the new network, otherwise we reject it. This procedure is then repeated for  $S$  proposed rewirings. In Fig. 2 we present the results of this rewiring algorithm for two experiments. We consider two networks: one with relatively homogeneous frequencies drawn from a unit normal distribution (left column) and a second with heterogeneous frequencies drawn from a symmetric power-law distribution,  $g(|\omega|) \sim |\omega|^{-3}$  (right column). Both networks contain  $N = 1000$  oscillators. In Figs. 2 (a) and (b) we plot the synchronization profiles for the initial networks and the networks obtained after  $2 \cdot 10^4$  rewirings. In both experiments, the rewired networks display better synchronization properties with sharp transitions from incoherence to strong synchronization. Each experiment is initialized with a different network topology: a SF network constructed by the configuration model with  $\gamma = 3$  and  $d_0 = 2$  and an Erdős-Rényi (ER) [27] network with average degree  $\langle d \rangle = 4$  are paired with the normally and power-law distributed frequencies, respectively. In Figs. 2 (c) and (d) we plot the initial and rewired degree distributions. In both experiments the degree distribution evolves

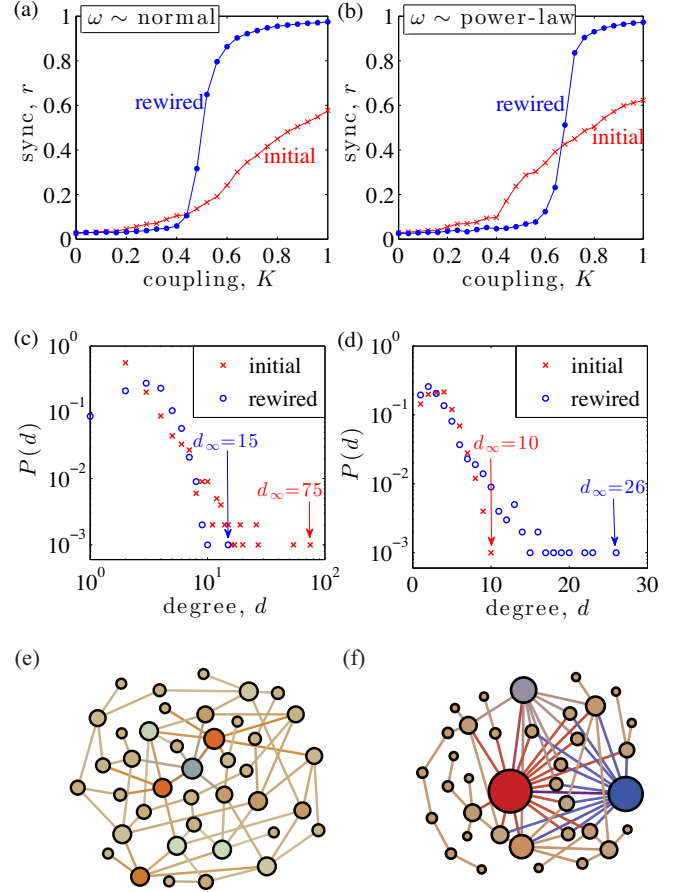


FIG. 2. (Color online) Network design: (a)-(b)  $r$  vs  $K$  for initial (red crosses) and rewired (blue circles) networks with normal and power-law distributed frequencies. (c)-(d) Degree distributions of the initial (red crosses) and rewired (blue circles) networks. (e)-(f) Illustrations for  $N = 40$  and  $36$  of networks after rewiring.

to better match that of the frequencies, either becoming less [Fig. 2(c)] or more [Fig. 2(d)] heterogeneous. This is further emphasized by the shifts in the maximal degrees  $d_\infty$ , which decreases from 75 to 15 for the normally distributed frequencies and increases from 10 to 26 for the power-law distributed frequencies. This suggests that for non-identical oscillators, a more heterogeneous network better synchronizes a more heterogeneous set of frequencies. To illustrate this phenomenon, we show in Figs. 2 (e) and (f) networks resulting from the same experiment with fewer nodes ( $N = 40$  and  $36$ , respectively). The radius of each node is proportional to its degree and the coloring of the node indicates its frequency from most positive (red) to most negative (blue). Here the phenomenon is easily observable with the emergence of network hubs in panel (f) but not (e). These hubs also have the largest frequencies in magnitude, suggesting positive degree-frequency correlations in optimal networks.

We now study in more detail the synchrony alignment function given in Eq. (7). Just as aligning  $\omega$  with  $v^N$  maximizes  $r$ , it follows that in the strong coupling regime, aligning  $\omega$  with other eigenvectors  $v^i$  of decreasing index yields



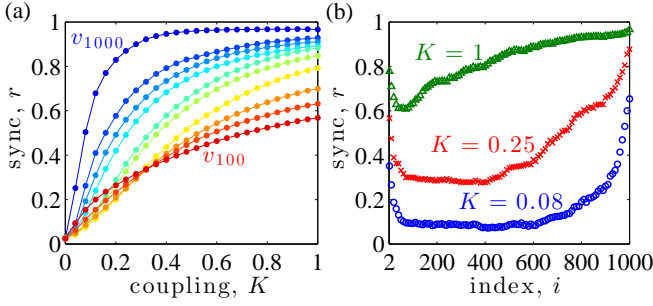


FIG. 3. (Color online) Eigenvector alignments: (a)  $r$  vs  $K$  for frequency alignments  $\omega \propto v^{100}, v^{200}, \dots, v^{1000}$  (red to blue). (b)  $r$  vs  $i$  for  $\omega \propto v^i$  with fixed  $K = 0.08$  (blue circles),  $0.25$  (red crosses), and  $1$  (green triangles). Each point is averaged over 50 SF network realization of size  $N = 1000$  with  $\gamma = 3$  and  $d_0 = 2$ .

weaker synchronization. We consider the alignments  $\omega \propto v^i$  and plot the synchronization profiles in Fig. 3 (a) for  $i = 100, 200, \dots, 1000$  (red to blue) averaged over 50 realizations of SF networks with parameters  $N = 1000$ ,  $\gamma = 3$ , and  $d_0 = 2$ . As expected, we observe weaker synchronization with decreasing index. We also plot in panel (b)  $r$  vs the index  $i$  for a few isolated coupling strengths:  $K = 0.08, 0.25$ , and  $1$ , again averaged over 50 realizations. For all three coupling strengths  $r$  tends to increase with  $i$ , provided  $i$  is not too small. For  $K = 0.08$  the majority of alignments yield incoherence with  $r$  undergoing a sharp increase only near the most dominant eigenvectors, while the increase in  $r$  is more gradual for  $K = 0.25$  and  $1$ . We also point out that for very small  $i$  we observe a short increase in  $r$ , which we attribute to local synchronization of different clusters in the network that yield large fluctuations in  $r$ .

Before concluding, we investigate the dynamical and structural properties present in optimized networks. In particular, we consider local degree-frequency and neighboring frequency-frequency correlations. In Fig. 4 (a) we plot the frequency magnitude  $|\omega_i|$  vs degree  $d_i$  for synchrony-optimized systems obtained from three methods: optimally chosen and optimally arranged frequencies for a fixed network, and an optimally rewired network for a fixed frequency vector. Networks are SF with  $N = 1000$ ,  $\gamma = 3$ , and  $d_0 = 3$  and frequencies for the arranged and rewired networks are normally distributed. In each case we observe a strong trend indicating a positive degree-frequency correlation, indicating that the largest frequencies correspond to the network hubs. Moreover, in Fig. 4 (b) we plot for each node  $i$  the average frequency of its neighboring oscillators  $\langle \omega \rangle_i = \sum_{j=1}^N A_{ij} \omega_j / d_i$  vs  $\omega_i$ . Correlations for the optimal choice (inset) are plotted using  $\log_{10} \omega = \text{sgn}(\omega) \log_{10} |\omega|$  for easier visualization. The results are qualitatively similar for each case, showing a strong negative correlation between neighboring frequencies. These observations agree with those of Refs. [28, 29], where similar positive and negative correlations were found to promote global synchronization. We finally note that such degree-frequency correlations may help explain the increased sharpness of transitions shown in Figs. 1 and 2 (a) and (b), since

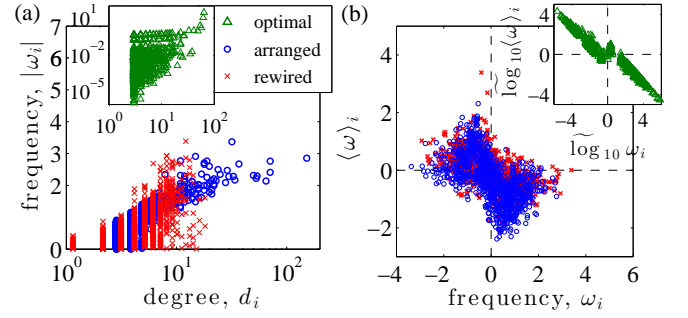


FIG. 4. (Color online) Correlations in optimized networks: (a) Frequency magnitude  $|\omega_i|$  vs degree  $d_i$  and (b) average neighbor frequency  $\langle \omega_i \rangle$  vs frequency  $\omega_i$  for networks with optimally chosen frequencies (green triangles), optimally arranged frequencies (blue circles), and an optimally rewired network (red crosses). Networks are SF with  $N = 1000$ ,  $\gamma = 3$ , and  $d_0 = 3$ . Frequencies for the arranged and rewired cases are normally distributed.

similar correlations can lead to discontinuous transitions [19].

In this Letter we have investigated the optimization of network synchronization. Our main result is the derivation of a synchrony alignment function that simultaneously encodes the network structure and oscillators' frequencies and allows for a systematic optimization of synchronization. We have demonstrated its utility with two general classes of optimization problem for the illustrative case of Kuramoto coupling. First, we considered constrained frequency allocation, where we found that synchronization is promoted by a strong alignment of the frequency vector with the most dominant Laplacian eigenvectors. Second, we considered network design, where we found that, relatively speaking, homogenous networks best synchronize homogenous frequencies, while heterogeneous networks best synchronize heterogeneous frequencies. In all cases we found that in optimized networks the large frequencies are localized to hubs and frequencies of neighboring oscillators are negatively correlated.

Finally, we contrast our results addressing heterogeneous oscillators to the well-developed theory addressing identical oscillators [30], for which the synchronizability of a network is given by the ratio  $\lambda_N / \lambda_2$  of network Laplacian eigenvalues [31] – a result allowing for optimization to be independent of the node dynamics [32]. In contrast, we find here that the synchronization of a network of heterogeneous oscillators generally depends on not only the full set of eigenvalues and eigenvectors of the network Laplacian, much like the case of nearly-identical oscillators [33] and synchronization in real-world experiments [34], but more importantly, how the network structure pairs with the heterogeneity of node dynamics (here oscillator frequencies). A network that is easily synchronizable with identical oscillators may have poor synchronization properties with heterogeneous oscillators, and vice-versa.

This work was funded in part by the James S. McDonnell Foundation (PSS), NSF Grant No. DMS-1127914 through the Statistical and Applied Mathematical Sciences Institute (DT), and ARO Grant No. 61386-EG (JS).

---

\* skardals@gmail.com

† dane.r.taylor@gmail.com

‡ sunj@clarkson.edu

- [1] S. H. Strogatz, *Sync: the Emerging Science of Spontaneous Order* (Hyperion, 2003).
- [2] A. Pikovsky, M. Rosenblum, and J. Kurths, *Synchronization: A Universal Concept in Nonlinear Sciences* (Cambridge University Press, 2003).
- [3] S. N. Dorogovtsev, A. V. Goltsev, and J. F. F. Mendes, *Rev. Mod. Phys.* **80**, 1275 (2008).
- [4] A. Arenas, A. Díaz-Guilera, J. Kurths, Y. Moreno, and C. Zhou, *Phys. Rep.* **469**, 93 (2008).
- [5] J. Buck, *Q. Rev. Biol.* **63**, 265 (1988).
- [6] L. Glass and M. C. Mackey, *From Clocks to Chaos: The Rhythms of Life* (Princeton University Press, Princeton, 1988).
- [7] A. E. Motter, S. A. Myers, M. Anghel, and T. Nishikawa, *Nat. Phys.* **9**, 191 (2013).
- [8] S. H. Strogatz, D. M. Abrams, A. McRobie, B. Eckhardt, and E. Ott, *Nature (London)* **438**, 43 (2005).
- [9] A. Prindle, P. Samayoa, I. Razinkov, T. Danino, L. S. Tsimring, and J. Hasty, *Nature* **481**, 39 (2012).
- [10] H. Daido, *Prog. Theor. Phys.* **88**, 1213 (1992).
- [11] Y. Kuramoto, *Chemical Oscillations, Waves, and Turbulence* (Springer, New York, 1984).
- [12] H. Sakaguchi and Y. Kuramoto, *Prog. Theor. Phys.* **76**, 576 (1986).
- [13] Y. Moreno and A. F. Pacheco, *Europhys. Lett.* **68**, 603 (2004).
- [14] T. Ichinomiya, *Phys. Rev. E* **70** 026116 (2004).
- [15] J. G. Restrepo, E. Ott, and B. R. Hunt, *Phys. Rev. E* **71**, 036151 (2005).
- [16] A. Arenas, A. Díaz-Guilera, and C. J. Pérez-Vicente, *Phys. Rev. Lett.* **96**, 114102 (2006).
- [17] J. Gómez-Gardeñes, Y. Moreno, and A. Arenas, *Phys. Rev. Lett.* **98**, 034101 (2007).
- [18] J. G. Restrepo, E. Ott, and B. R. Hunt, *Phys. Rev. E* **76**, 056119 (2007).
- [19] J. Gómez-Gardeñes, S. Gómez, A. Arenas, and Y. Moreno, *Phys. Rev. Lett.* **106** 128701 (2011).
- [20] P. S. Skardal and J. G. Restrepo, *Phys. Rev. E* **85**, 016208 (2012).
- [21] P. S. Skardal and J. G. Restrepo, Proceedings of the 2012 International Symposium on Nonlinear Theory and its Applications. October 22-26, 2012, Palma, Mallorca, Spain.
- [22] P. S. Skardal, J. Sun, D. Taylor, and J. G. Restrepo, *Europhys. Lett.* **101**, 20001 (2013).
- [23] F. Dörfler, M. Chertkov, and F. Bullo, *Proc. Natl. Acad. Sci.* **110**, 2005 (2013).
- [24] A. Ben-Israel and T. N. E. Grenville, *Generalized Inverses* (Springer, New York, 1974).
- [25] A. Bekessy, P. Bekessy, and J. Komlos, *Stud. Sci. Math. Hung.* **7**, 343 (1972).
- [26] I. J. Farkas, I. Derényi, A.-L. Barabási, and T. Vicsek, *Phys. Rev. E* **64**, 026704 (2001).
- [27] P. Erdős and A. Rényi, *Pub. Math. Inst. Hung. Acad. Sci.* **5**, 17 (1960).
- [28] M. Brede, *Phys. Lett. A* **372**, 2618 (2008).
- [29] L. Buzna, S. Lozano, and A. Díaz-Guilera, *Phys. Rev. E* **80**, 066120 (2009).
- [30] L. M. Pecora and T. L. Carroll, *Phys. Rev. Lett.* **80**, 2109 (1998).
- [31] M. Barahona and L. M. Pecora, *Phys. Rev. Lett.* **89**, 054101 (2002).
- [32] T. Nishikawa and A.E. Motter, *Proc. Natl. Acad. Sci. U.S.A.* **107**, 10 342 (2010).
- [33] J. Sun, E. M. Bollt, and T. Nishikawa, *Europhys. Lett.* **85**, 60011 (2009).
- [34] B. Ravoori, A. B. Cohen, J. Sun, A. E. Motter, T. E. Murphy, and R. Roy, *Phys. Rev. Lett.* **107**, 034102 (2011).